CVR-2018-299

Supplemental Material

Immune cell census in murine atherosclerosis: cytometry by time of flight illuminates vascular myeloid cell diversity

Jennifer E Cole[1]*, Inhye Park[1]*, David Ahern[1], Christina Kassiteridi[1], Dina Danso Abeam[1], Michael Goddard[1], Patricia Green[1], Pasquale Maffia[2,3,4], Claudia Monaco[1]

[1]Kennedy Institute of Rheumatology, Nuffield Department of Orthopaedics, Rheumatology and Musculoskeletal Sciences, University of Oxford, Oxford, United Kingdom;
[2]Centre for Immunobiology, Institute of Infection, Immunity and Inflammation, College of Medical, Veterinary and Life Sciences, University of Glasgow, Glasgow, United Kingdom;
[3]Institute of Cardiovascular and Medical Sciences, College of Medical, Veterinary and Life Sciences, University of Glasgow, Glasgow, United Kingdom;
[4]Department of Pharmacy, University of Naples Federico II, Naples, Italy.

* These authors contributed equally

Corresponding author
Professor Claudia Monaco
Kennedy Institute of Rheumatology
Roosevelt Drive
Headington
Oxford, OX3 7FY
United Kingdom
E-mail:claudia.monaco@kennedy.ox.ac.uk
Tel:+44 1865 612636
Fax:+44 1865 612601

Supplemental Table 1: List of antibody clones used in CyTOF analysis

Metal Label	Antigen	Clone	Manufacturer	Conjugation	Figures used in for clustering
141Pr	Ly-6G/C (Gr-1)	RB6-8C5	Fluidigm	Fluidigm	1-3, 5
142Nd	CD11c	N418	Fluidigm	Fluidigm	1-3, 5
143Nd	IL7Ra	A7R34	Biolegend	In-house	1,2, S2, S3
144Nd	XCR1	ZET	Biolegend	In-house	1-3, 5
145Nd	TCRgd	GL3	Biolegend	In-house	1, 2, S2
146Nd	CX3CR1	SA011F11	Biolegend	In-house	1-3, 5, S3
147Sm	CD45	30-F11	Fluidigm	Fluidigm	None
148Nd	CD11b (Mac-1)	M1/70	Fluidigm	Fluidigm	1-3, 5
149Sm	CD19	6D5	Fluidigm	Fluidigm	1, 2
150Nd	CD24	M1/69	Fluidigm	Fluidigm	1-3, 5, S3
151Eu	CD64	X54-5/7.1	Fluidigm	Fluidigm	1-3, 5
152Sm	CD3e	145-2C11	Fluidigm	Fluidigm	1, 2
153Eu	CD335(NKp46)	29A1.4	Fluidigm	Fluidigm	1, 2
154Sm	CD31 (PECAM-1)	390	Abcam	In-house	None
155Gd	ACTA 2	1A4	Sigma	In-house	None
156Gd	CD169	3D6.112	Biolegend	In-house	1-3, 5
158Gd	CD206	C068C2	Biolegend	In-house	1-3, 5
159Tb	F4/80	BM8	Fluidigm	Fluidigm	1-3, 5
160Gd	CD26	DPP-4	Biolegend	In-house	1-3, 5, S2, S3
161Dy	CD103	2E7	Biolegend	In-house	1-3, 5, S2, S3
162Dy	Ly6C	HK1.4	Fluidigm	Fluidigm	1-3, 5, S2, S3
163Dy	CCR2	SA203G11	Biolegend	In-house	1-3, 5, S2, S3
164Dy	CD172a	SIRPa	Biolegend	In-house	1-3, 5, S2, S3
165Ho	CD161 (NK1.1)	PK136	Fluidigm	Fluidigm	1, 2, S2
166Er	CD209b (SIGNR1)	2C7B27	Biolegend	In-house	1-3, 5
167Er	SIGLECF	E50-2440	BD	In-house	1-3, 5
168Er	CD8a	53-6.7	Fluidigm	Fluidigm	1, 2, S2
169Tm	TCRb	H57-597	Fluidigm	Fluidigm	1, 2, S2
170Er	CD90.2	30-H12	Biolegend	In-house	1-3, 5
171Yb	CD44	IM7	Fluidigm	Fluidigm	1-3, 5, S2, S3
172Yb	CD4	RM4-5	Fluidigm	Fluidigm	1, 2, S2
173Yb	SIGLECH	551	Biolegend	In-house	1, 2
174Yb	I-A/I-E (MHCII)	M5/114.15.2	Fluidigm	Fluidigm	3, 5
175Lu	CD68	FA-11	Biolegend	In-house	1-3, 5
176Yb	CD45R (B220)	RA3-6B2	Fluidigm	Fluidigm	1, 2, S3

Supplemental Table 2: Baseline composition of aortas from chow and high fat diet fed ApoE-/- mice

Diet	Live (% of cells) mean ± SD	p (vs chow)	CD45+ (% of Live cells)	p (vs chow)
Chow	85.6 ± 3.9	-	35.1 ± 5.0	-
High Fat	87.2 ± 4.7	ns	38.4 ± 4.1	ns

Supplemental Table 3: Percentage of Myeloid and T cells

Diet	Myeloid (% of CD45+ cells) mean ± SD	p (vs chow)	CD90.2+CD3+ (% of CD45+ cells) mean ± SD	p (vs chow)
Chow	75.58 ± 5.0	-	7.97 ± 2.35	-
High Fat	76.35 ± 6.3	ns	8.49 ± 2.35	ns

Supplemental Figures and Legends

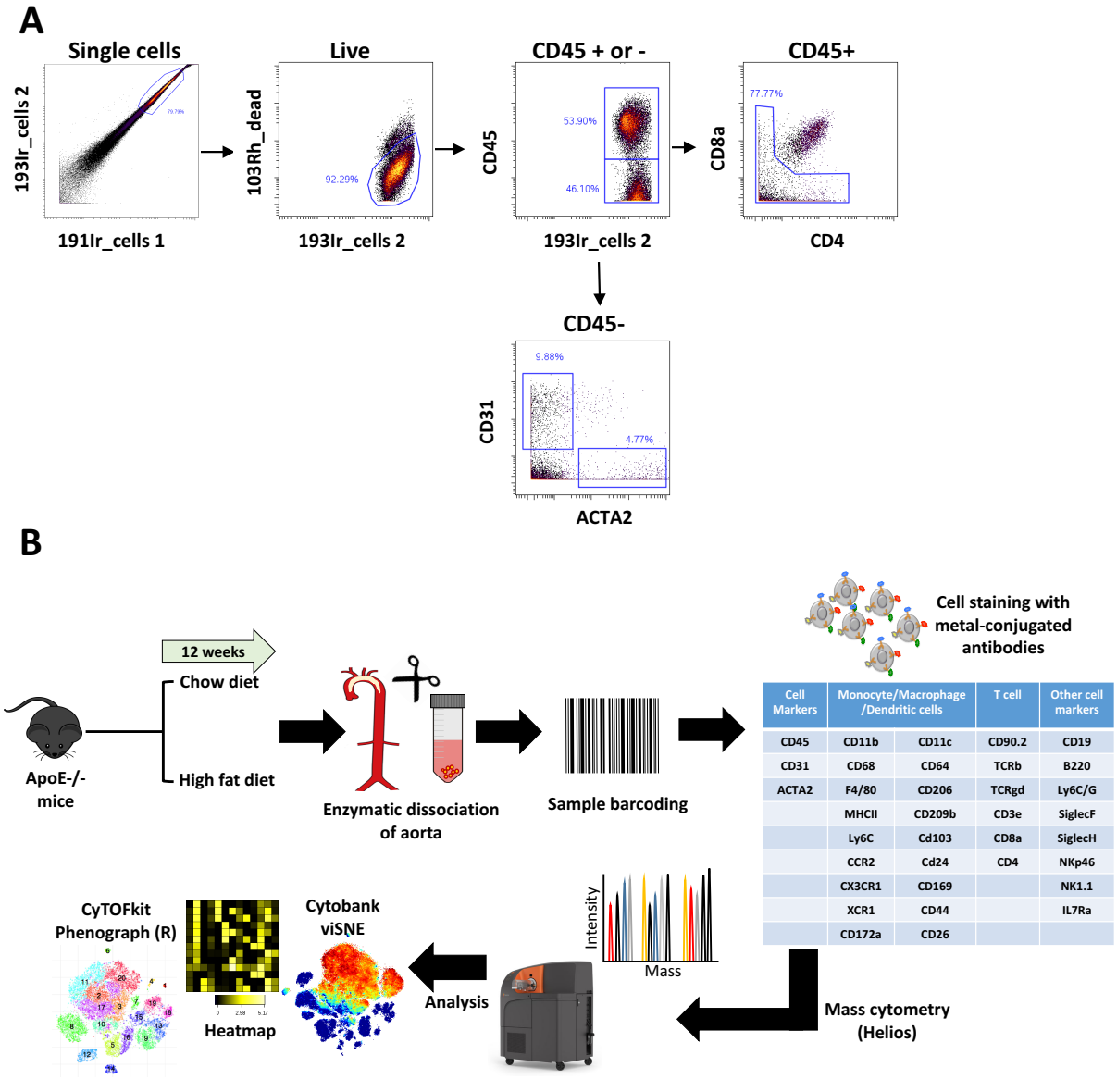

Figure S1 Gating strategy for Live CD45+ leucocytes and schematic illustration of experimental design. A. Iridium DNA intercalator double positive events were gated as cells and normalisation beads were removed. Rhodium DNA intercalator negative cells were gated as live cells, which were then separated by the expression of CD45. $CD45^+$ cells were regarded as leucocytes and $CD45^-$ populations were further gated by CD31 and alpha smooth muscle cell actin 2 (ACTA2). $CD45^-CD31^+$ and $CD45^-ACTA2^+$ cells can be identified as endothelial cells and smooth muscle cells, respectively. To reduce thymic contamination, $CD45^+CD4^+CD8^+$ populations were removed from analyses. **B** Apolipoprotein E-deficient (ApoE-/-) mice were fed a chow or high fat diet at the age of 12-week for 12 weeks. Aortas were collected from the mice and single cells obtained by enzymatic digestion. Cells then underwent barcoding and staining using a panel of 35 cell markers (supplemental table 1). Data from the stained cells were acquired using Helios and were analysed using Cytobank (viSNE and heatmap) and CyTOFkit phenograph.

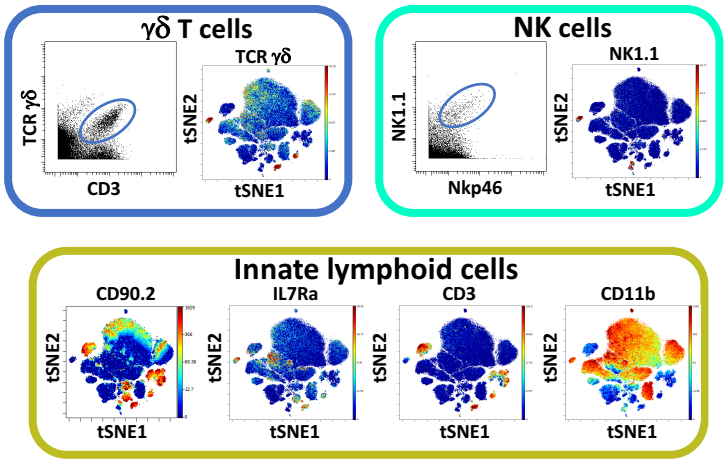

Figure S2 Identification of leucocyte populations in aortas of ApoE-/- mice. Single cell suspensions of aortas from Apolipoprotein E-deficient (ApoE-/-) mice fed either a chow or high fat diet were stained with a panel of 35 antibodies. For each sample, cells from 2 aortas were pooled. Live $CD45^{+}$ cells concatenated from the aortas of all apolipoprotein E-deficient (ApoE-/-) mice studied (both chow and high fat fed) (n=13) were clustered using viSNE on expression of 35 cell surface and intracellular markers outlined in supplemental table 1. The analysis identifies 15 populations including myeloid, lymphocyte and unknown subsets (Figure 1). The selected populations are displayed in a viSNE dot plot showing the expression level of their major markers with or without a representative dot plot showing two relevant cell population markers.

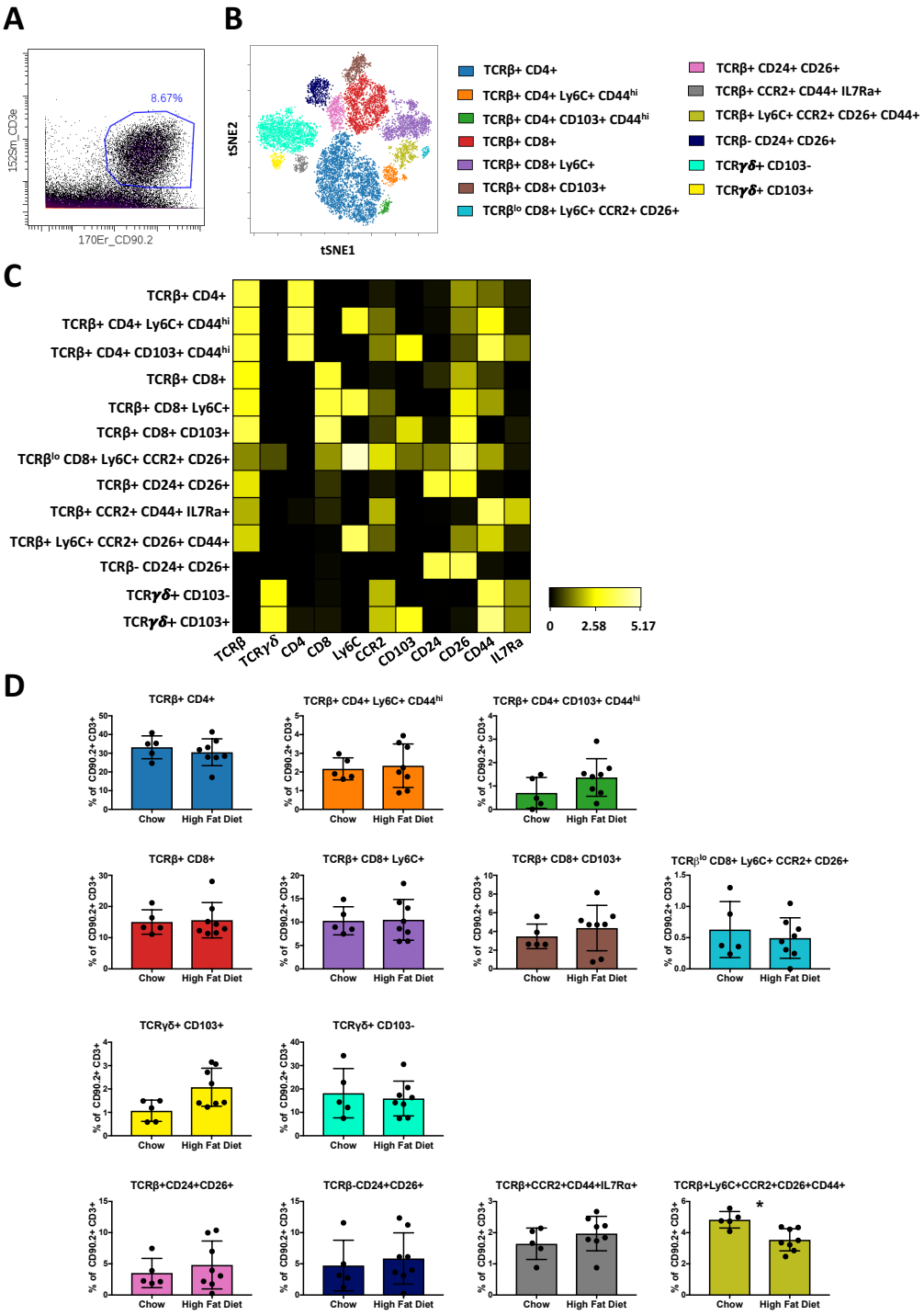

Figure S3 viSNE analysis reveals multiple T lymphocyte subsets in murine atherosclerotic aortas. A. Dot plot showing T cells gating ($CD3e^{+}CD90.2^{+}$ from live $Lin^{-}CD45^{+}$ leucocytes). **B.** T lymphocytes were clustered using viSNE on the expression of 12 cell surface and intracellular markers outlined in supplemental table 1. Identification of the 13 cell population clusters which included 3 $CD4^{+}$ T cells, 3 $CD8^{+}$ T cells, 2 γδ T cells and 5 unknown populations. **C.** Heatmap showing the relative expression level of 11 cell markers within the 13 T cell subsets identified by the viSNE clustering shown in B. **D.** Bargraphs showing the changes in abundance of the cell populations identified in the viSNE clustering outlined in B, between chow and high fat diet fed mice. Data are presented as Mean± SD, Dots represent individual samples, n=5-8 *P<0.05

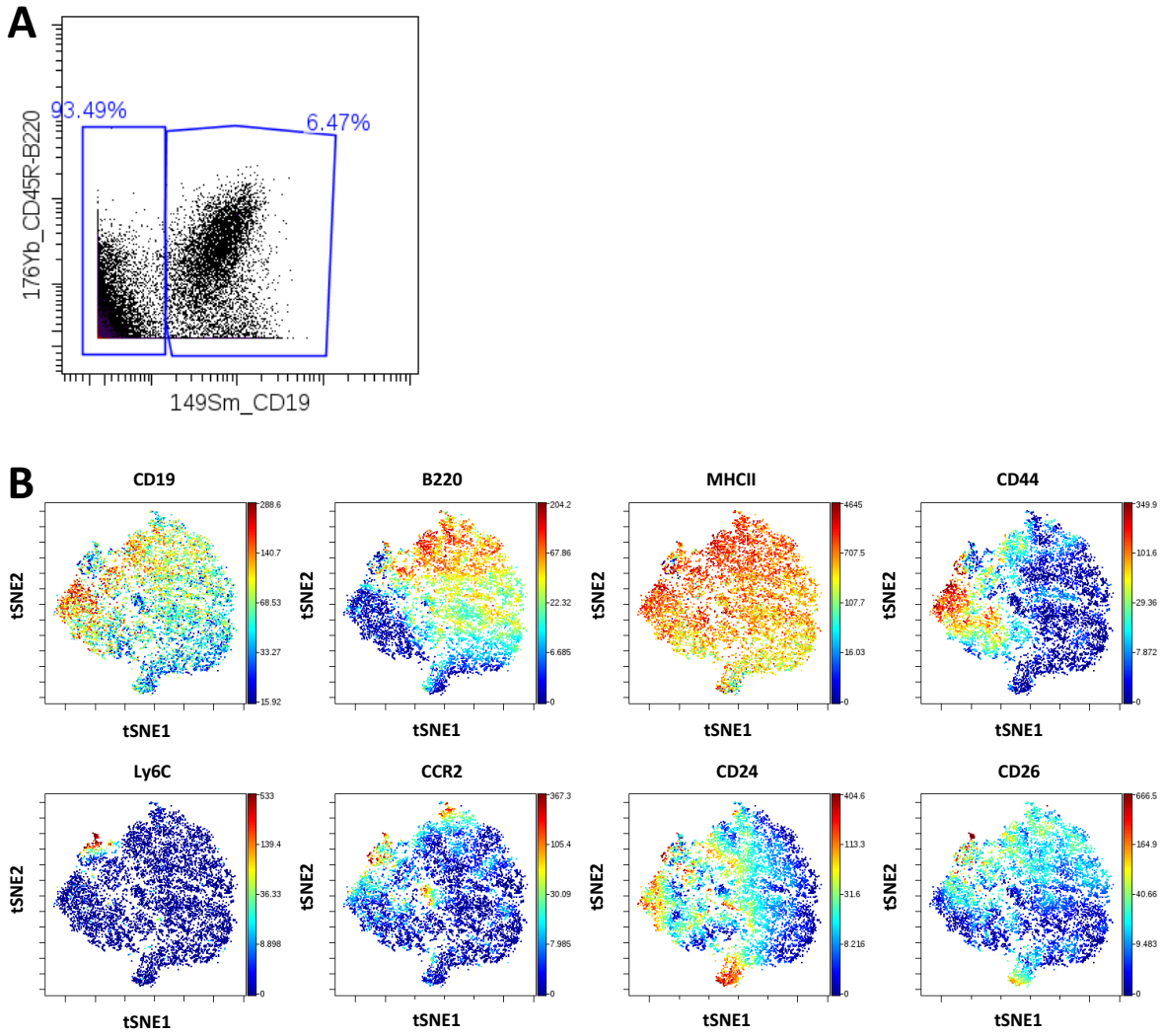

Figure S4 B cells exhibit different expression profiles of key markers. A. Dot plot showing B cells gating ($CD19^{+}B220^{-/+}$ from live Lin-CD45+ leucocytes). **B.** B cells were clustered using viSNE on the expression of 10 cell surface and intracellular markers outlined in supplemental table 1. Expression levels of selected myeloid markers in the resulting viSNE clustered cell populations is shown.

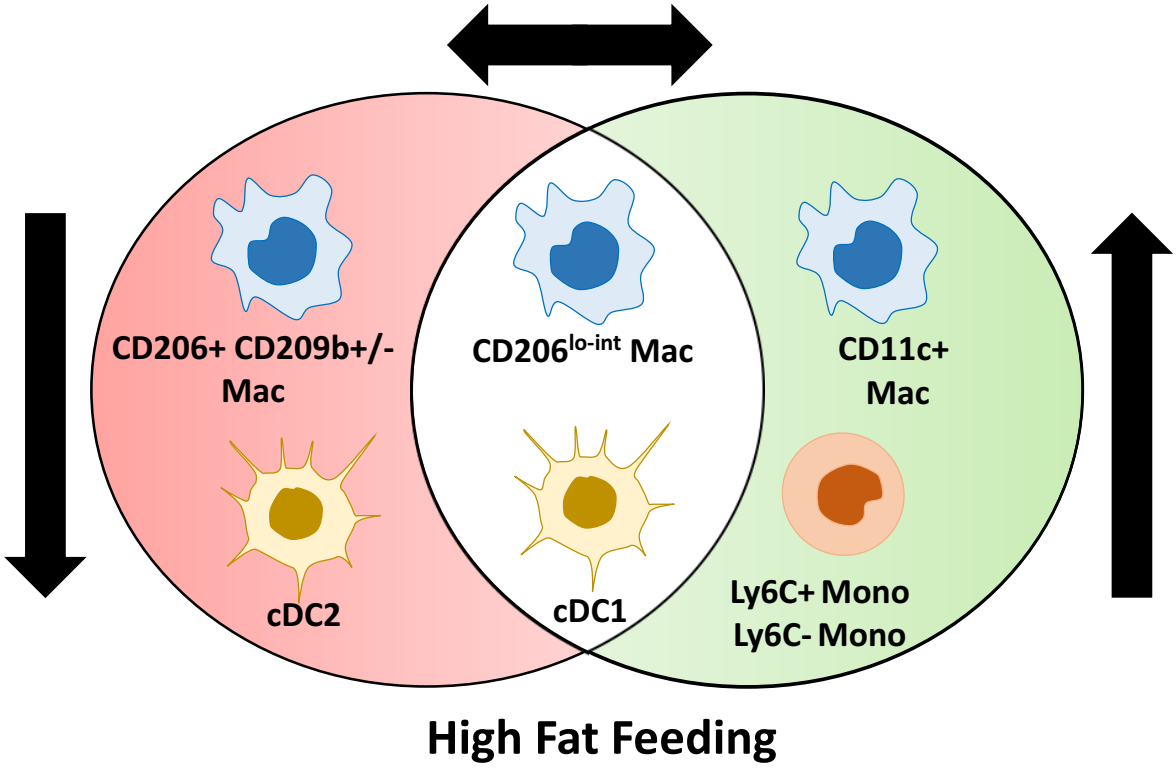

Figure S5 Schematic diagram showing how myeloid cell populations in atherosclerotic aortas of ApoE-/- mice are affected by high fat feeding. High fat feeding of ApoE-/- mice induces changes in the proportion of several myeloid cell subsets in the aorta as identified by viSNE analysis. $Ly6C^{+}$ and $Ly6C^{-}$ monocytes as well as $CD11c^{+}$ macrophages were increased in aortas of high fat fed mice (green circle) and conventional type 2 dendritic cells (cDC2) and $CD206^{+}CD169^{+}CD209^{+/-}$ macrophages were reduced (red circle). Proportions of conventional type 1 dendritic cells (cDC1), and $CD206^{lo\text{-}int}$ subsets were unchanged by high fat feeding.